

This document is confidential and is proprietary to the American Chemical Society and its authors. Do not copy or disclose without written permission. If you have received this item in error, notify the sender and delete all copies.

Charge-Transfer Emission in Oligotriarylamine-Triarylborane Compounds

Journal:	<i>The Journal of Organic Chemistry</i>
Manuscript ID:	jo-2015-00416t.R1
Manuscript Type:	Article
Date Submitted by the Author:	16-Mar-2015
Complete List of Authors:	Bonn, Annabell; University of Basel, Department of Chemistry Wenger, Oliver; University of Basel, Department of Chemistry

SCHOLARONE™
Manuscripts

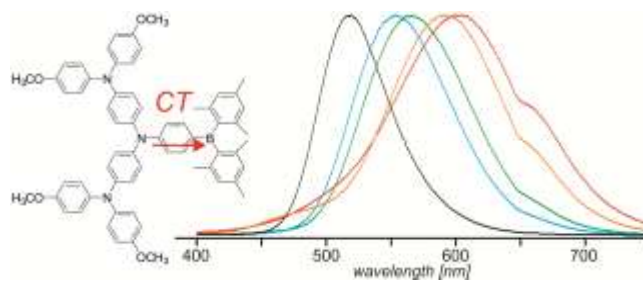
Charge-Transfer Emission in Oligotriarylamine-Triarylborane Compounds

*Annabell G. Bonn and Oliver S. Wenger**

Department of Chemistry, University of Basel, St. Johannis-Ring 19, CH-4056 Basel,

Switzerland

Email: oliver.wenger@unibas.ch



1
2
3 ABSTRACT
4
5
6

7 Donor-acceptor compounds exhibiting charge transfer emission are of interest in a variety of
8 different contexts, for example for nonlinear optical processes and for sensor applications.
9
10 Recently investigated triarylamine-triarylborane compounds represent an important class of
11 donor-acceptor systems, and we explored to what extent their charge-transfer properties can be
12 further improved by using stronger amine donors and borane acceptors than prior studies. The
13 oligotriarylamine employed here is a much stronger donor than previously used triarylamines
14 containing single nitrogen centers. In order to increase the acceptor strength, the electron-
15 accepting unit was equipped with two (instead of one) dimesitylboron substituents. In our
16 comparative study, six donor-acceptor compounds were synthesized and investigated by cyclic
17 voltammetry and optical spectroscopy. An increase of the donor strength through replacement of
18 an ordinary triarylamine by an oligotriarylamine unit leads to the expected energetic stabilization
19 of charge transfer (CT) excited states but the emission solvatochromism is not more pronounced.
20
21 The attempted increase of the acceptor strength by substitution of the acceptor moiety by two
22 (instead of one) dimesitylboron groups leads to a drastic decrease of emission quantum yields.
23
24 Based on these results, our purely experimental study provides fundamental guidelines for the
25 design of new triarylamine-triarylborane donor-acceptor compounds with favorable charge-
26 transfer emission properties.
27
28
29
30
31
32
33
34
35
36
37
38
39
40
41
42
43
44
45
46
47
48
49
50
51
52
53
54
55
56
57
58
59
60

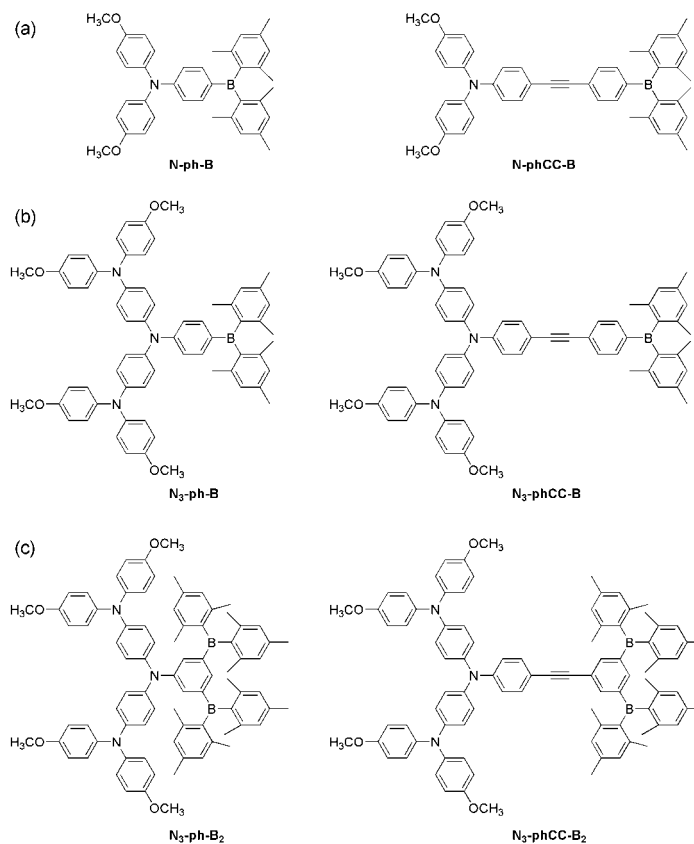
1
2
3 INTRODUCTION
4
5

6 Donor-acceptor compounds have fascinated chemists for many decades, but research on such
7 molecules remains an important topic even nowadays because donor-acceptor compounds find
8 application in many different areas. For example, many recently developed organic dyes for solar
9 cells are donor-acceptor compounds.¹ For imaging, luminescent donor-acceptor compounds are
10 of great current interest, because two-photon absorption followed by charge transfer emission
11 can be used to convert two near-infrared input photons into one visible output photon.² Other
12 donor-acceptor compounds are explored in the context of sensor materials, or, when part of
13 conjugated oligomers or polymers, for light-emitting diodes and charge transfer networks in
14 general.^{2b, 3} For fundamental studies, investigation of discrete donor-acceptor molecules in
15 solution with UV-Vis absorption, photoluminescence, and cyclic voltammetry remains a
16 valuable experimental approach.
17
18
19
20
21
22
23
24
25
26
27
28
29
30
31

32 4-(Dimethylamino)benzonitrile (DMABN) and its derivatives are among the best known
33 examples of donor-acceptor compounds,⁴ but in recent years attention has shifted to other types
34 of systems. An important class of relatively new donor-acceptor compounds is comprised of
35 triarylamine donor and triarylborane acceptor moieties, linked together covalently via π -
36 conjugated molecular bridges.⁵ Some of these triarylamine-triarylborane systems have been
37 employed as molecular sensors which are selective for fluoride and cyanide;⁶ the detection
38 process is often based on a change in optical absorption or emission due to a shift of charge
39 transfer (CT) states upon anion binding at the triarylborane.^{6e, 7} In other cases, the motivation for
40 study of triarylamine-triarylborane compounds came from the interest in new luminescent
41 materials or from a fundamental interest the CT process.⁸ Compounds with multiple arylamine
42 donor / arylborane acceptor sites have also been explored.⁹
43
44
45
46
47
48
49
50
51
52
53
54
55
56
57
58
59
60

1
2
3 The aim of this project was to explore whether the favorable CT properties of triarylamine-
4 triarylborane compounds could be further improved by making the donor and acceptor groups
5 even stronger while keeping the donor-acceptor distance relatively short. Toward this end, we
6 performed a comparative study of the CT behavior of “traditional” triarylamine-triarylborane
7 compounds (N-ph-B, N-phCC-B; Scheme 1a) and two molecules with an oligotriarylamine
8 donor and a triarylborane acceptor (N₃-ph-B, N₃-phCC-B; Scheme 1b). The oligotriarylamine is
9 known to have significantly lower oxidation potentials than ordinary triarylamines,¹⁰ i. e., it is a
10 substantially stronger electron donor than ordinary triarylamines with single N centers. In an
11 attempt to probe the additional effect resulting from an increase of acceptor strength, two
12 compounds equipped with two dimesitylboron centers (N₃-ph-B₂, N₃-phCC-B₂; Scheme 1c) were
13 investigated. The rationale for this acceptor design is that the presence of two electron-deficient
14 boron substituents will increase the reduction potential of the acceptor, i. e., make it easier to
15 reduce. This, however, necessitates attachment of the boron atoms in *meta*-position to the amine
16 donor.

17
18
19
20
21
22
23
24
25
26
27
28
29
30
31
32
33
34
35
36 Our study is of purely experimental nature as the purpose of this work was to establish guiding
37 principles for the molecular design of new triarylamine-triarylborane donor-acceptor compounds
38 with favorable CT emission properties, based on phenomenological observations.
39
40
41
42
43
44
45
46
47
48
49
50
51
52
53
54
55
56
57
58
59
60

Scheme 1. Molecular structures of the donor-acceptor compounds investigated in this work.

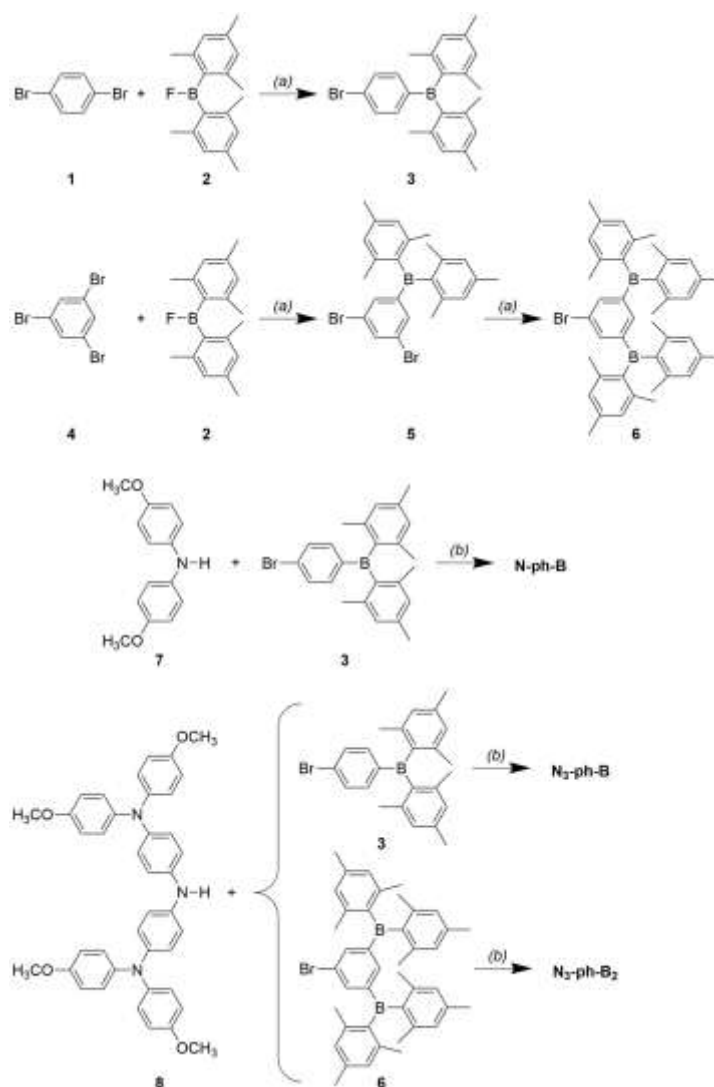
RESULTS AND DISCUSSION

Synthesis. The acceptor moieties were synthesized by reacting 1,4-dibromobenzene (**1**) or 1,3,5-tribromobenzene (**4**) with dimesitylboron fluoride (**2**), yielding compounds **3**,¹¹ **5**,¹² and **6** (Scheme 2).¹³ **3** and **6** were coupled to dianisylamine (**7**) or an equivalent oligotriarylamine building block (**8**)^{10c} to afford N-ph-B, N₃-ph-B, and N₃-ph-B₂. For the second series of donor-acceptor compounds, the starting point was 4-bromo-1-iodobenzene (**9**) which was coupled to trimethylsilyl acetylene (**10**) to result in compound **11** (Scheme 3).¹⁴ The latter was reacted with the abovementioned amines **7** or **8** in Pd-catalyzed N-C coupling reactions yielding compounds

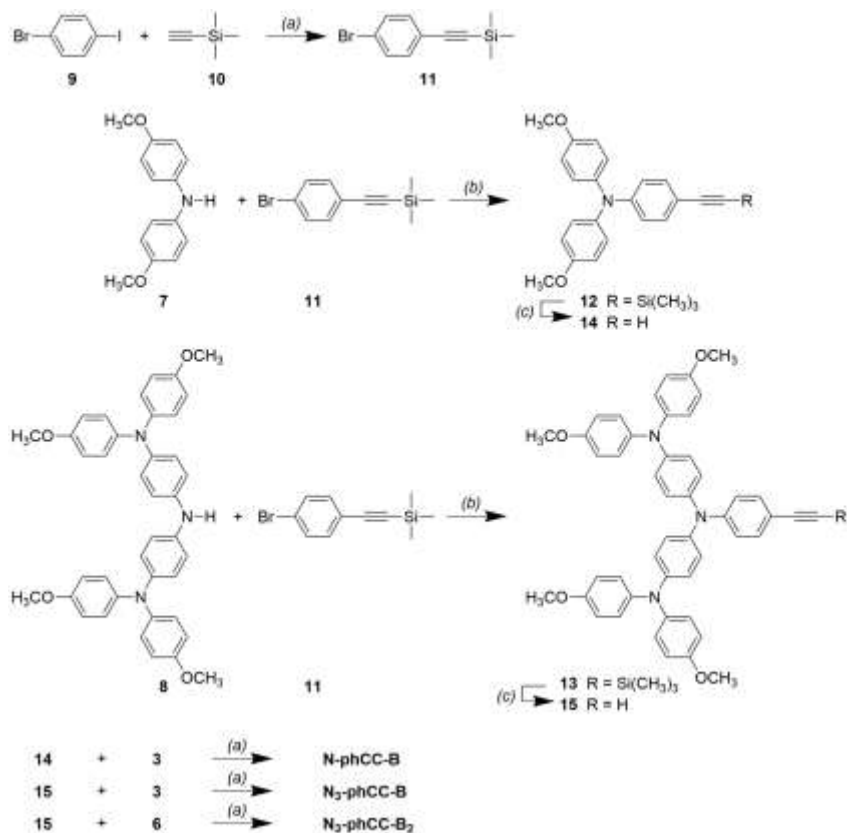
1
2
3
4
5
6
7
8
9
10
11
12
13
14
15
16
17
18
19
20
21
22
23
24
25
26
27
28
29
30
31
32
33
34
35
36
37
38
39
40
41
42
43
44
45
46
47
48
49
50
51
52
53
54
55
56
57
58
59
60

12 and **13**.¹⁵ Deprotection of the trimethylsilyl groups resulted in the acetylene compounds **14** and **15** which were reacted with the borane building blocks **3** or **6** to afford N-phCC-B,^{9b} N₃-phCC-B, and N₃-phCC-B₂.

Scheme 2. Synthesis of donor-acceptor compounds; (a) *n*-BuLi, Et₂O, -78 °C; (b) Pd(dba)₂, NaO^tBu, (HP^tBu₃)BF₄, toluene, reflux. For single reaction steps, the yields of the individual compounds were: **3**, 80%; **5**, 69%; **6**, 69%; N-ph-B, 92%; N₃-ph-B, 77%; N₃-ph-B₂, 63%.



Scheme 3. Synthesis of donor-acceptor compounds; (a) $\text{PdCl}_2(\text{PPh}_3)_2$, CuI , Et_3N , reflux; (b) $\text{Pd}(\text{dba})_2$, NaO^tBu , $(\text{HP}^t\text{Bu}_3)\text{BF}_4$, toluene, reflux; (c) TBAF, THF, 25 °C. For single reaction steps, the yields of the individual compounds were: **11**, ~100%; **12**, 64%; **13**, 74%; **14**, 99%; **15**, 91%; N-phCC-B, 43%; N_3 -phCC-B, 42%; N_3 -phCC-B₂, 34%.



Electrochemistry. Cyclic voltammetry was used to measure the electrochemical potentials for donor oxidation and acceptor reduction in the 6 compounds from Scheme 1. In Figure 1 the voltammograms for N-ph-B, N_3 -ph-B, and N_3 -ph-B₂ measured in dry and de-oxygenated THF at 25 °C in presence of 0.1 M TBAPF₆ are shown. Oxidation of the triarylamine moiety of N-ph-B (Figure 1a) occurs at 0.33 V vs. Fc^+/Fc while reduction of the triarylborane unit takes place at -2.75 V vs. Fc^+/Fc (Table 1). Both potentials are in line with previously reported values for

1
2
3 comparable compounds.¹⁶ Oxidation of the oligotriarylamine donor in N₃-ph-B to its
4 monocationic form occurs at -0.02 V vs. Fc⁺/Fc (Figure 1b) and the dication is formed at 0.15 V
5 vs. Fc⁺/Fc. At higher potentials, oxidation of the third N center is commonly observed in
6 oligotriarylaminines,¹⁰ but this is often an irreversible process, and it occurs outside the potential
7 window considered in Figure 1. For the CT emission properties of our donor-acceptor
8 compounds only oxidation of the first N center is relevant because the lowest-energy CT state
9 involves only the electron in the energetically highest orbital. This first oxidation occurs at the
10 central N atom of the oligotriarylamine because this is the most electron-rich position.^{10a} CT
11 excitations at higher energies may of course involve the peripheral, less readily oxidizable N
12 atoms, but these states are not emissive. From the data in Figure 1 and Table 1 we conclude that
13 oligotriarylamine is a stronger one-electron donor than the ordinary triarylamine by ~0.35 eV.
14 This is markedly different from what can be achieved in simple NAr₂ donors (Ar = C₆H₄R; R =
15 H, OMe, etc.); in this regard the oligotriarylamine used here is special.
16
17
18
19
20
21
22
23
24
25
26
27
28
29
30
31
32
33

34 The triarylborane reduction potential is only marginally affected by the change in amine
35 between N-ph-B and N₃-ph-B (Table 1). However, when the acceptor moiety is equipped with
36 two boron centers (N₃-ph-B₂) its reduction potential shifts to less negative values by about 0.2 V
37 (Figure 1c, Table 1). Intuitively this makes sense because two electron-withdrawing
38 dimesitylboron groups will lead to a less electron-rich compound than only one dimesitylboron
39 substituent. On the other hand, in N₃-ph-B₂ the dimesitylboron groups are electronically more
40 decoupled from the amino-unit than in N-ph-B or in N₃-ph-B because the respective electro-
41 active groups are in *meta*- rather than *para*-position to each other. Donation of electron density
42 from the amino-groups towards the boron atoms is therefore expected to be weaker in N₃-ph-B₂
43 than in N-ph-B and in N₃-ph-B, and this could also lead to a shift of the dimesitylboron-related
44
45
46
47
48
49
50
51
52
53
54
55
56
57
58
59
60

reduction potential to less negative values. It is not a priori clear which one of these two effects has a dominant influence or whether they both contribute to similar extents. Obviously, a reference molecule equipped with only one dimesitylboron-substituent in *meta*-position to the amino-group would be useful to address this question, but this is beyond the scope of the present study. For our purposes it is sufficient to note that reduction of N₃-ph-B₂ occurs more easily by ca. 0.2 V than reduction of N-ph-B and N₃-ph-B.

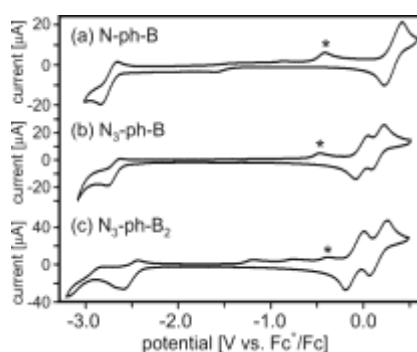


Figure 1. Cyclic voltammograms measured for (a) N-ph-B, (b) N₃-ph-B, (c) N₃-ph-B₂ in dry and de-oxygenated THF with 0.1 M TBAPF₆. The potential sweep rate was 0.1 V/s in all cases. The waves marked with an asterisk (*) were only detected after an initial oxidative sweep to potentials more positive than 0.5 V vs. Fc⁺/Fc and are attributed to electrochemical side products.

Table 1. Electrochemical potentials (in Volts vs. Fc⁺/Fc) for oxidation of amine-based donor moieties and for reduction of triarylborane-based acceptor moieties in the compounds from Scheme 1 in THF.^a ΔG^0 is the free energy for electron transfer from amine to borane calculated as $\Delta G^0 \approx e \cdot [E(\text{amine}^{+/0}) - E(\text{borane}^{-/0})]$.^b E_{CT} is the energetic position of the CT emission band

maximum in hexane. E_{00} is the energy of the electronic origin of the emissive CT state, estimated from the emission onsets.

	$E(\text{amine}^{+/0})$	$E(\text{amine}^{2+/+})$	$E(\text{borane}^{0/-})$	ΔG_{CT}^0 [eV]	E_{CT} [eV]	E_{00} [eV]
N-ph-B	0.33		-2.75	3.08	2.73	3.05
N ₃ -ph-B	-0.02	0.15	-2.69	2.67	2.39	2.74
N ₃ -ph-B ₂	-0.09	0.17	-2.52	2.43	2.11	2.64
N-phCC-B	0.29		-2.37	2.66	2.80	3.03
N ₃ -phCC-B	-0.06	0.12	-2.36	2.30	2.44	2.82
N ₃ -phCC-B ₂	-0.06	0.16	-2.48	2.42	2.68	2.98

^a Extracted from the data in Figure 1 and Figure S1; measured in presence of 0.1 M TBAPF₆, using dry and de-oxygenated solvent and potential sweep rates of 0.1 V/s. ^b This free energy may be regarded as a measure for the energy of the optical N→B charge transfer, see text.

Regarding donor oxidation, completely analogous observations are made for the series of compounds containing additional ethynyl spacers (N-phCC-B, N₃-phCC-B, N₃-phCC-B₂); the respective voltammograms are shown in Figure S1. Triarylborane reduction is easier by ~0.4 V in N-phCC-B and N₃-phCC-B compared to their analogs without ethynyl spacers (N-ph-B, N₃-ph-B). Attachment of a second boron center to the acceptor site (in compound N₃-phCC-B₂) does not result in a further increase of the reduction potential.

For each compound, the free energy for electron transfer (ΔG_{CT}^0) from the amine donor to the borane acceptor can be estimated using the relation $\Delta G^0 \approx e \cdot [E(\text{amine}^{+/0}) - E(\text{borane}^{0/-})]$, leading to the values in the fifth column of Table 1 (e is the elemental charge). The respective free energies do not directly correspond to the expected optical CT energies (E_{CT}) because the latter involve Franck-Condon transitions between excited states and vibrationally unrelaxed ground

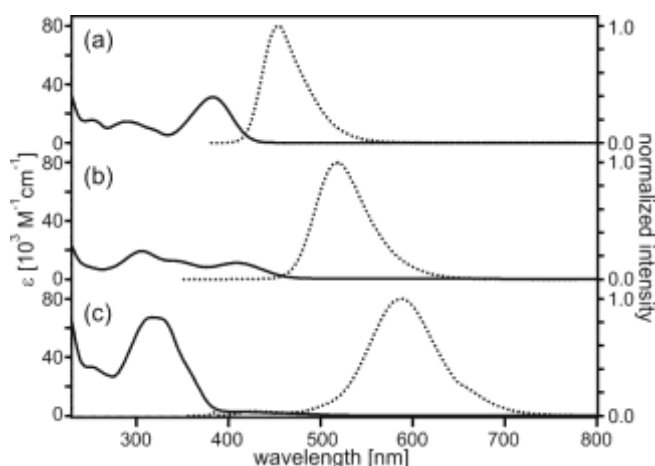
1
2
3 states. However, within a homologous series of compounds the estimated ΔG_{CT}^0 values should at
4
5
6 least reflect the trends in optical CT energies. Inspection of Table 1 shows that this is indeed the
7
8 case. The E_{CT} values in Table 1 were derived from emission band maxima. A more correct
9
10 treatment would be based on the energies of the electronic origins of the CT absorption and
11
12 emission bands (E_{00}), but from room-temperature solution spectra the respective energies can
13
14 only be determined with large uncertainties. In the last column of Table 1 we report E_{00} values
15
16 estimated on the basis of emission band onsets. Expectedly, E_{00} and E_{CT} follow the same trend
17
18 because the excited-state distortions are similar in all compounds considered here, and
19
20 consequently the correlation between ΔG_{CT}^0 and E_{00} is equally good as the correlation between
21
22 ΔG_{CT}^0 and E_{CT} within a given series of compounds.
23
24
25
26
27
28
29

30 *Optical absorption and emission spectroscopy in hexane.* In Figure 2 the UV-Vis absorption
31
32 (solid lines) and luminescence spectra (dotted lines) of (a) N-ph-B, (b) N₃-ph-B, and (c) N₃-ph-
33
34 B₂ in hexane at 25 °C are shown. Under these conditions, the lowest-energy absorption band
35
36 maxima are at 383 nm for N-ph-B and at 410 nm for N₃-ph-B, and these bands are attributed to
37
38 CT transitions. In the spectrum of N₃-ph-B₂ there is an intense band with a maximum at 321 nm,
39
40 but this is not the lowest-energy absorption. The intense band at 321 nm is attributed to a π - π^*
41
42 transition while the CT transition is merely observable as a shoulder between 400 and 550 nm
43
44 (Figure S2).
45
46
47
48

49 In the case of N₃-ph-B₂ CT absorption is comparatively weak due to poor electronic coupling
50
51 between the amine donor and the dimesitylboron-substituents which are connected to the
52
53 bridging phenylene unit in *meta*- rather than *para*-position. The oscillator strength is proportional
54
55 to the squared electronic coupling matrix element, hence even a relatively small decrease in
56
57
58
59
60

1
2
3 donor-acceptor coupling strength can entail a substantial decrease in extinction. It is well known
4 that electronic couplings between *meta*-substituents at phenylene bridging units are significantly
5 weaker than electronic couplings between *para*-substituents. In this regard, our finding of weak
6 CT absorption in N₃-ph-B₂ is not at all surprising; the rationale for this *meta*-substitution pattern
7 is described in the Introduction.
8
9

10
11 The emission band maxima of N-ph-B, N₃-ph-B, and N₃-ph-B₂ in hexane at 25 °C occur at
12 454, 518, and 587 nm and thus follow the trend predicted for CT energies based on the
13 electrochemical data (fifth column of Table 1).
14
15
16
17
18
19
20
21
22
23



24
25
26
27
28
29
30
31
32
33
34
35
36
37
38
39
40
41 **Figure 2.** UV-Vis absorption (solid lines) and normalized luminescence spectra (dotted lines) of
42 (a) N-ph-B ($\lambda_{\text{exc}} = 370$ nm), (b) N₃-ph-B ($\lambda_{\text{exc}} = 330$ nm), (c) N₃-ph-B₂ ($\lambda_{\text{exc}} = 345$ nm) in hexane
43 at 25 °C. (λ_{exc} denotes the excitation wavelength).
44
45
46
47
48
49
50

51 For the series of compounds with additional ethynyl-linkers (right part of Scheme 1) similar
52 absorption and emission behavior is observed. The key difference is that the CT emission
53 maxima follow a different trend than for the compounds without ethynyl-linkers (Figure S3),
54
55
56
57
58
59
60

1
2
3 increasing in wavelength from 443 to 508 nm between N-phCC-B and N₃-phCC-B but then
4
5 decreasing to 462 nm for N₃-phCC-B₂. However, this trend follows exactly the prediction made
6
7 on the basis of the electrochemical data (last two columns of Table 1).
8
9

10
11 *Solvatochromism and changes in dipole moment.* In Figure 3a the CT emission of N-ph-B in
12
13 five different solvents at 25 °C is shown. The focus was set on hexane, toluene, diethyl ether,
14
15 THF and CH₂Cl₂ for all six compounds from Scheme 1, because in these solvents luminescence
16
17 quantum yields are above 3% in most cases. Solvents of higher polarity (e. g., acetone, DMF,
18
19 DMSO) lead to lower luminescence quantum yields, and it becomes difficult to distinguish
20
21 between luminescence emitted by the compounds under study and artifacts. As the solvent
22
23 polarity increases there is a pronounced red-shift of the emission, as expected for this class of
24
25 compounds.^{8c, 17} For N-ph-B the solvatochromic shift of the band maximum amounts to 3050
26
27 cm⁻¹ between hexane and CH₂Cl₂ (Figure 3a), and for N₃-ph-B it is 2720 cm⁻¹ (Figure 3b). The
28
29 N₃-ph-B₂ compound only emits significantly in hexane (Figure 3c). Positive solvatochromism is
30
31 also observed for the emission of N-phCC-B, N₃-phCC-B, and N₃-phCC-B₂ (Figure S4). The
32
33 latter two compounds only emit significantly in hexane, toluene, and diethyl ether hence the shift
34
35 in emission band maxima between hexane and diethyl ether is a useful measure for comparison
36
37 of solvatochromism in the molecules from the right half of Scheme 1. For N-phCC-B the
38
39 respective shift is 3000 cm⁻¹, for N₃-phCC-B it is 2760 cm⁻¹, and for N₃-phCC-B₂ we detect 3720
40
41 cm⁻¹. With the exception of N₃-phCC-B₂, emission solvatochromism is not more pronounced in
42
43 the oligotriarylamine-triarylborane compounds than in the reference molecules containing
44
45 ordinary triarylamine donors with single nitrogen centers (N-ph-B, N-phCC-B).
46
47
48
49
50
51
52
53
54
55
56
57
58
59
60

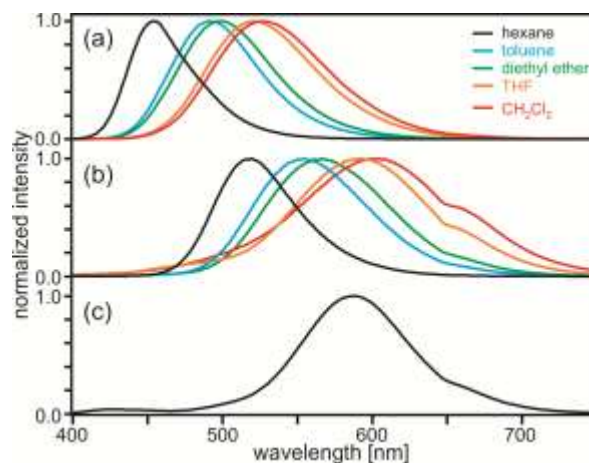


Figure 3. Normalized photoluminescence of (a) N-ph-B, (b) N₃-ph-B, and (c) N₃-ph-B₂ in various solvents at 25 °C. Excitation wavelengths (λ_{exc}) were as follows: 370 nm for N-ph-B, 330 nm for N₃-ph-B, and 345 nm for N₃-ph-B₂. The kink at 650 nm in the spectra from panels (b) and (c) is an artifact caused by the instrument.

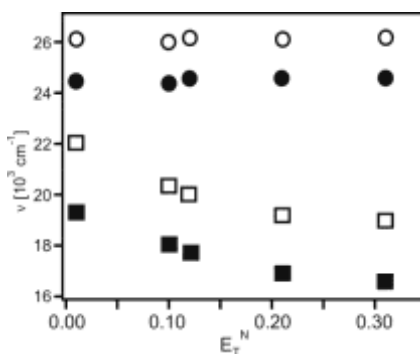


Figure 4. Absorption (circles) and emission band maxima (squares) as a function of solvent polarity (expressed in the form of Reichardt parameters).¹⁸ Open circles and squares: N-ph-B; filled circles and squares: N₃-ph-B.

In optical absorption spectroscopy hardly any solvatochromism is detected for all compounds from Scheme 1 (Figure S5 and Figure S6). This is not unexpected because the electronic ground

state is associated with a substantially weaker dipole moment than the CT excited state.^{8g, 17a} In Figure 4 the CT absorption and emission band maxima of N-ph-B and N₃-ph-B are plotted as a function of solvent polarity (expressed in the form of Reichhardt parameters);¹⁸ analogous plots for N-phCC-B, N₃-phCC-B, and N₃-phCC-B₂ are shown in Figure S7. It is evident from these plots that solvatochromism is far more pronounced in emission than in absorption.

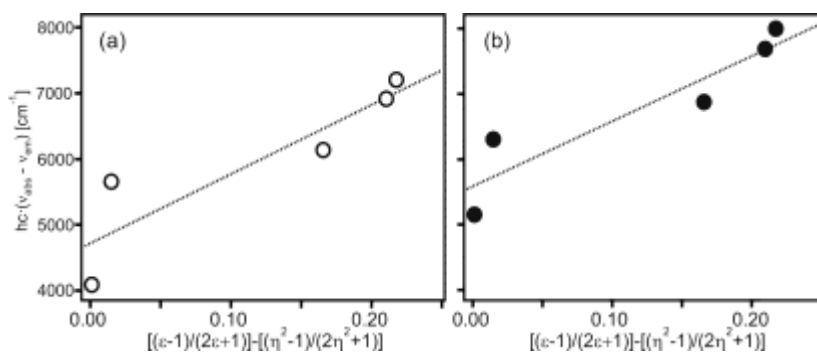


Figure 5. Lippert-Mataga plot showing the dependence of Stokes shift between CT absorption and emission on solvent polarity for (a) N-ph-B and (b) N₃-ph-B.

As an alternative to the Reichhardt parameter plots, the method by Lippert and Mataga is frequently employed for analysis of the solvent-dependence of absorption and emission bands.¹⁹ This method permits estimation of the difference between ground- and excited-state dipole moments ($\Delta\mu_{eg}$) from the dependence of the Stokes shift on solvent polarity (eq. 1).

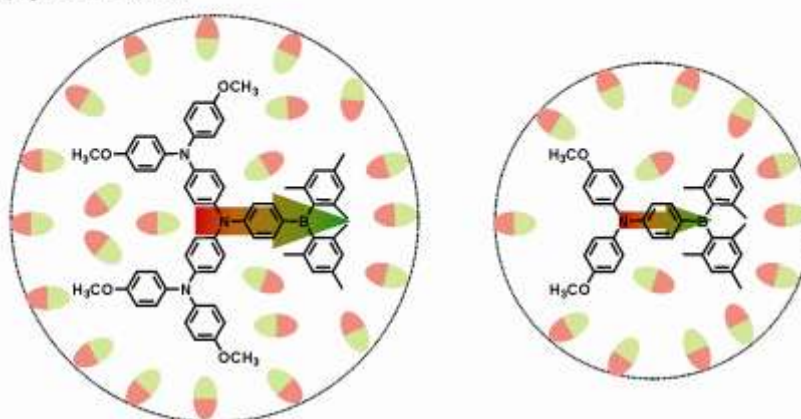
$$hc \cdot (v_{abs} - v_{em}) = hc \cdot (v_{abs}^{vac} - v_{em}^{vac}) \cdot \frac{2 \cdot (\Delta\mu_{eg})^2}{a_0^3} \cdot \left[\frac{\epsilon - 1}{2\epsilon + 1} - \frac{\eta^2 - 1}{2\eta^2 + 1} \right] \quad (\text{eq. 1})$$

1
2
3 In equation 1, the solvent polarity is captured by the $(\epsilon-1)/(2\epsilon+1) - (\eta^2-1)\cdot(2\eta^2+1)$ term in
4
5 which ϵ is the dielectric constant and η is the refractive index.¹⁹ The $hc\cdot(v_{\text{abs}} - v_{\text{em}})$ and $hc\cdot(v_{\text{abs}}^{\text{vac}}$
6
7 $- v_{\text{em}}^{\text{vac}})$ terms are the differences in absorption and emission maxima in a given solvent and in
8
9 vacuum, respectively. In our cases, these are simply the Stokes shifts for the CT transition in a
10
11 given solvent and in vacuum, and $hc\cdot(v_{\text{abs}} - v_{\text{em}})$ can readily be determined from our
12
13 experimental data in Figures 3, S4, S5, and S6. In Figure 5 we show plots of $hc\cdot(v_{\text{abs}} - v_{\text{em}})$
14
15 versus $(\epsilon-1)/(2\epsilon+1) - (\eta^2-1)\cdot(2\eta^2+1)$ for N-ph-B (a) and N₃-ph-B (b). Linear regression fits yield
16
17 $hc\cdot(v_{\text{abs}}^{\text{vac}} - v_{\text{em}}^{\text{vac}})$ from the intercept and $2\cdot\Delta\mu_{\text{eg}}^2 / a_0^3$ from the slope; the parameter a_0 is the so-
18
19 called Onsager radius of the solvent cavity formed around the chromophore.²⁰ The key outcome
20
21 from this analysis is that the slope (i. e., the ratio of $2\cdot\Delta\mu_{\text{eg}}^2$ and a_0^3) is within experimental
22
23 accuracy the same for N-ph-B ($10500\pm 3000 \text{ cm}^{-1}$) and N₃-ph-B ($10000\pm 2300 \text{ cm}^{-1}$). Estimation
24
25 of the Onsager radius is usually associated with significant uncertainty, and even small errors in
26
27 a_0 will have a large impact on the estimated value for $\Delta\mu_{\text{eg}}$ when attempting to extract dipole
28
29 moment changes from $2\cdot\Delta\mu_{\text{eg}}^2 / a_0^3$ ratios.^{17a, 21} Furthermore, it is usually debatable to what
30
31 extent the solvent cavity can indeed be approximated as spherical. In view of these limitations
32
33 and the relatively modest linear correlations found in Figure 5 ($R^2 = 0.81$ and 0.86 , respectively),
34
35 it seems appropriate to simply make the following semi-quantitative point: When going from N-
36
37 ph-B to N₃-ph-B the increase in molecular size may well be associated with a 25% increase in
38
39 Onsager radius. Such a relatively modest increase in a_0 can completely mask a 40% increase in
40
41 $\Delta\mu_{\text{eg}}$. In other words, CT in N₃-ph-B is indeed likely to be associated with a significantly
42
43 increased change in dipole moment when compared to N-ph-B. However, this anticipated and
44
45 desired effect is outbalanced by the increase in Onsager radius, and the net result is similar
46
47 solvatochromism in N₃-ph-B and N-ph-B. This key outcome is graphically summarized in
48
49
50
51
52
53
54
55
56
57
58
59
60

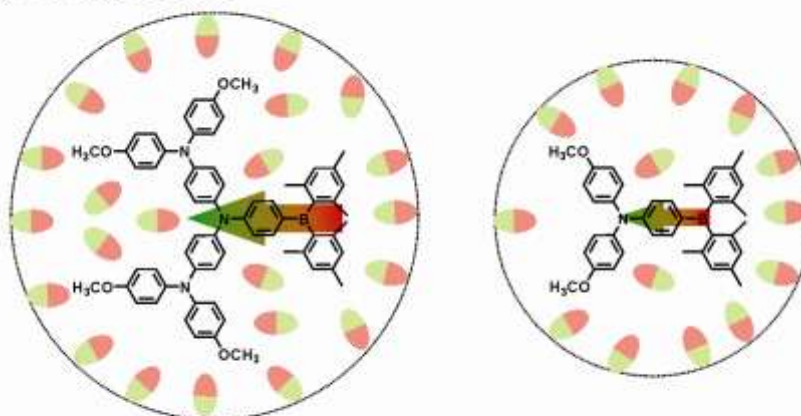
Scheme 4. Keeping the molecular size small while increasing the push-pull character is therefore an important guiding principle for the design of future triarylamine-triarylborane compounds, at least when aiming at strong solvatochromism.

Scheme 4. Illustration of ground- and excited-state dipole moments (arrows in the centers) in N_3 -ph-B (left) and N-ph-B (right) and solvent dipole moments (elliptical objects) with Onsager radii (a_0 ; dotted circles).

(a) ground state



(b) CT excited state



larger $\Delta\mu_{eg}$
larger a_0

smaller $\Delta\mu_{eg}$
smaller a_0



similar ratio of $\Delta\mu_{eg}$ and a_0
→ similar solvatochromism



Luminescence quantum yields and lifetimes. The luminescence quantum yields of the individual donor-acceptor compounds from Scheme 1 correlate reasonably well with the energetic position of the emission band maximum (Table 2). As the CT excited state shifts to lower energies, luminescence quantum yields tend to decrease. This behavior is compatible with the so-called energy gap law which states that nonradiative relaxation processes become increasingly efficient with decreasing energy gap between emissive excited state and ground state (or energetically next lower-lying excited state).²² However, there is no clear correlation between quantum yields and excited state lifetimes, suggesting that both radiative and nonradiative excited-state decay rates vary substantially from one solvent to the other. The efficiency of nonradiative relaxation processes is notoriously difficult to rationalize, but one possibility is that interactions between solvent donor molecules and the dimesitylboron acceptor groups provide an efficient thermal relaxation pathway. This effect could become increasingly efficient with increasing solvent polarity. On the other hand the boron center is relatively well shielded from its chemical environment due to the bulky mesityl-substituents.

Table 2. Luminescence quantum yields (ϕ) and lifetimes (τ) in aerated solvents at 25 °C.

cmpd	hexane		toluene		diethyl ether		THF		CH ₂ Cl ₂	
	ϕ	τ /ns	ϕ	τ /ns	ϕ	τ /ns	ϕ	τ /ns	ϕ	τ /ns
N-ph-B	0.59	4.1	0.72	6.0	0.75	7.4	0.63	7.6	0.66	8.6
N ₃ -ph-B	0.49	5.8	0.50	7.8	0.40	7.0	0.12	2.7	0.04	1.1
N ₃ -ph-B ₂	0.06	11.8								
N-phCC-B	0.81	1.8	0.85	2.6	0.88	3.6	0.49	2.8	0.38	2.4
N ₃ -phCC-B	0.63	3.6	0.52	4.1	0.11	1.8				
N ₃ -phCC-B ₂	0.21	3.8	0.13	9.3	0.08	13.2				

1
2
3
4
5
6
7 While N-ph-B, N₃-ph-B, and N-phCC-B exhibit strong CT emission in all 5 solvents
8
9 considered here, the doubly dimesitylboron-substituted compounds N₃-ph-B₂ and N₃-phCC-B₂
10
11 exhibit poor luminescence properties. Twofold boron-substitution of the acceptor group was
12
13 motivated by an increase in acceptor strength, but this requires attachment of the dimesitylboron
14
15 groups in *meta*-position relative to the N donor atom. As noted above, this entails a substantial
16
17 decrease of the oscillator strength associated with CT absorption in N₃-ph-B₂ and N₃-phCC-B₂
18
19 compared to the other compounds from Scheme 1 in which N and B atoms are in *para*-position
20
21 relative to each other. This effect has implications for the emission behavior of N₃-ph-B₂ and N₃-
22
23 phCC-B₂ because radiative decay rate constants are inversely proportional to oscillator strengths.
24
25 Thus, because of their weaker donor-acceptor coupling caused by the *meta*-linkage, N₃-ph-B₂
26
27 and N₃-phCC-B₂ do not only exhibit weaker CT absorption but they also have lower radiative
28
29 decay rate constants from the CT state. Moreover, if interaction between solvent donor
30
31 molecules and the dimesitylboron acceptor groups indeed provide an efficient thermal relaxation
32
33 pathway as suspected above, then one might argue that this effect is amplified in the presence of
34
35 two (instead of one) acceptor groups. Consequently, there are two effects that both can contribute
36
37 to the low luminescence quantum yields of N₃-ph-B₂ and N₃-phCC-B₂: (i) a decrease of radiative
38
39 excited-state decay rate constants and (ii) an increase of nonradiative excited-state decay rate
40
41 constants.
42
43
44
45
46
47
48

49 Another noteworthy observation from Table 2 is that luminescence quantum yields are lower
50
51 in N₃-ph-B than in N-ph-B (and similarly in N₃-phCC-B compared to N-phCC-B). Thus, the use
52
53 of an oligotriarylamine donor in place of a simple triarylamine has a negative influence on the
54
55 luminescence properties, particularly with increasing solvent polarity. The oscillator strengths for
56
57
58
59
60

1
2
3 CT absorptions are similar in these 4 compounds in all 5 solvents considered here (Figures S5
4 and S6), hence there is no physical basis for assuming that the radiative decay rate constants for
5 CT emission would be much different between these compounds in this range of solvents.
6
7
8 Consequently, the observed differences in quantum yields are most likely due to differences in
9 nonradiative excited-state relaxation. Two aspects seem important in this regard: (i)
10 oligotriarylamines are made of more atoms than simple triarylamines, and hence the number of
11 vibrational degrees of freedom is greater in N₃-ph-B and N₃-phCC-B than in N-ph-B and N-
12 phCC-B; (ii) the CT states are ~0.4 eV lower in energy in N₃-ph-B and N₃-phCC-B compared to
13 N-ph-B and N-phCC-B (Table 1). Lower luminescence quantum yields in the oligotriaryamine
14 systems are therefore in line with the energy gap law. As the emissive CT state is energetically
15 further stabilized by increasing solvent polarity, multiphonon relaxation becomes increasingly
16 efficient, and this effect is particularly dramatic for N₃-ph-B and N₃-phCC-B because in these
17 cases the CT energy in the more polar solvents approaches only 5-6 quanta of C-H stretching
18 vibrations. At least in so-called “weak coupling” cases (i. e., in systems in which there are only
19 small distortions between ground- and excited-states) this is typically the limit when
20 multiphonon relaxation begins to dominate. It is commonly the highest-frequency vibration of a
21 molecular system which is relevant because this is the most efficient promoter of energy
22 dissipation, hence our reference to C-H stretching vibrations. Thus, the lower luminescence
23 quantum yields of N₃-ph-B and N₃-phCC-B with respect to N-ph-B and N-phCC-B can be
24 understood on relatively simple grounds.
25
26
27
28
29
30
31
32
33
34
35
36
37
38
39
40
41
42
43
44
45
46
47
48
49

50 Finally we note that the N-phCC-B and N₃-phCC-B compounds have slightly higher
51 luminescence quantum yields than N-ph-B and N₃-ph-B, i. e., introduction of the ethynyl-linker
52 has a mildly beneficial influence on the luminescence properties, but only in the most apolar
53
54
55
56
57
58
59
60

1
2
3 solvents hexane and toluene (and diethyl ether in the case of N-phCC-B / N-ph-B). This is a
4 comparatively subtle effect which most likely has its origin in different nonradiative excited-state
5 relaxation rates; the relevant CT absorptions have similar oscillator strengths regardless of
6 whether ethynyl linkers are present or not (Figures S5, S6) hence the radiative excited-state
7 decay rates are likely to be largely unaffected by this change of linker. As a guiding principle for
8 the molecular design of new emissive triarylamine-triarylborane compounds it can be stated that
9 ethynyl-linkers have a mildly beneficial influence on luminescence quantum yields in strongly
10 apolar solvents but they become detrimental in even very weakly polar solvents such as THF and
11 CH₂Cl₂. Clearly, the influence of the ethynyl-linker on luminescence quantum yields is weak
12 compared to the influence of twofold dimesitylboron substitution and replacement of ordinary
13 triarylamine by oligotriarylamine (see above).
14
15
16
17
18
19
20
21
22
23
24
25
26
27
28
29
30
31
32
33

34 SUMMARY AND CONCLUSIONS

35
36
37
38

39 The aim of this study was to explore the potential for improvement of CT emission properties
40 of triarylamine-triarylborane donor-acceptor compounds from a purely experimental point of
41 view and to establish guiding principles for the molecular design of new systems of this type. All
42 key observations and trends observed for the 6 compounds from Scheme 1 can be adequately
43 rationalized on the basis of simple physicochemical principles. The key findings from this study
44 are:
45
46
47
48
49
50
51

52 (i) Trends in CT energies of unknown triarylamine-triarylborane compounds can be predicted
53 based on electrochemical potentials of the individual donor and acceptor components.
54
55
56
57
58
59
60

1
2
3 (ii) Oligotriarylaminines lead to the expected red-shift of CT emission because they are
4 substantially stronger donors than simple triarylaminines, but the increase in molecular size entails
5 a larger solvent cavity, i. e., more solvent dipole moments oppose the dipole moment change
6 associated with CT in the donor-acceptor molecule. The net result is a solvatochromic effect of
7 similar magnitude as with ordinary triarylaminines because the increase in dipole moment change
8 upon CT excitation is compensated by an increase in Onsager radius.
9

10
11 (iii) The attempted increase of acceptor strength by twofold dimesitylboron-substitution is a
12 failure in several regards. First, the effect on the acceptor reduction potential is relatively small.
13 Second, twofold substitution forcedly occurs in *meta*-position to the amine donor, and this
14 lowers the oscillator strength of the CT absorption considerably due to weaker electronic
15 coupling between the donor and the acceptor, and more importantly, it lowers radiative decay
16 rate constants from the CT excited states. Low CT luminescence quantum yields result.
17

18 (iv) Luminescence quantum yields with oligotriarylamine donors are somewhat lower than
19 with simple triarylaminines due to more efficient multiphonon relaxation processes.
20

21 From these key findings, the following guiding principles for the design of future systems with
22 amine donor and borane acceptor groups emerge:
23

24 (i) Size matters: When modifying the donor and/or acceptor groups in an attempt to enhance
25 the CT properties, it is desirable to keep the overall molecular size as small as possible.
26

27 (ii) The radiative decay rate for the CT excited state must be kept large by providing strong
28 electronic coupling between the donor and acceptor groups. *P*-phenylene and *p*-phenylene
29 ethynylene linkers behave similarly in this regard.
30

31 (iii) Very electron-rich triarylaminines which are smaller than the oligotriarylamine used here
32 would be desirable.
33
34
35
36
37
38
39
40
41
42
43
44
45
46
47
48
49
50
51
52
53
54
55
56
57
58
59
60

(iv) An increase in acceptor strength is better performed by fluorination of dimesitylboron units than by increasing the number of dimesitylboron-substituents.²³

EXPERIMENTAL SECTION

Compound **3**.¹¹ 1,4-Dibromobenzene (**1**) (1.75 g, 7.42 mmol) was dissolved in dry Et₂O (20 ml) under N₂. After cooling to -78 °C *n*-BuLi in hexane was added dropwise (3.40 ml, 5.44 mmol), and the mixture was stirred at this temperature for 3 h. A solution of dimesitylboron fluoride (**2**) (1.56 g, 5.82 mmol) in dry Et₂O was added dropwise and the suspension was stirred at room temperature overnight. Et₂O (50 ml) was added, and the organic phase was washed with saturated aqueous NH₄Cl solution (100 ml) and with water. After drying over anhydrous Na₂SO₄ and subsequent evaporation of the solvent, the raw product was purified by column chromatography on silica gel using pentane as the eluent. The pure product was obtained as a white solid (2.49 g, 6.15 mmol, 80%). ¹H NMR (400 MHz, CDCl₃): δ [ppm] 7.43 (ABq, 4 H, Δδ_{AB} = 0.02, J_{AB} = 8.0 Hz), 6.82 (s, 4 H), 2.31 (s, 6 H), 1.99 (s, 12 H).

Compound **5**.¹² 1,3,5-Tribromobenzene (**4**) (2.00 g, 6.35 mmol) was dissolved in dry Et₂O (30 ml) under N₂ and cooled to -78 °C. *n*-BuLi in hexane (2.54 ml, 6.35 mmol) was added dropwise, and the reaction mixture was stirred at -78 °C for 2 h. Dimesitylboron fluoride (**2**) (1.70 g, 6.35 mmol) was added, and the suspension was stirred at room temperature for 1 h. Then the solution was diluted with hexane (100 ml), washed with water and dried over Na₂SO₄. Chromatography on silica gel column with pentane gave the pure product as a white solid (2.12 g, 4.38 mmol, 69%). ¹H NMR (400 MHz, CDCl₃): δ [ppm] 7.76 (t, J = 1.9 Hz, 1 H), 7.51 (d, J = 1.9 Hz, 2 H), 6.82 (s, 4 H), 2.31 (s, 6 H), 1.97 (s, 12 H).

1
2
3
4
5
6
7
8
9
10
11
12
13
14
15
16
17
18
19
20
21
22
23
24
25
26
27
28
29
30
31
32
33
34
35
36
37
38
39
40
41
42
43
44
45
46
47
48
49
50
51
52
53
54
55
56
57
58
59
60

Compound **6**.¹³ Compound **5** (2.10 g, 4.34 mmol)¹² was reacted with *n*-BuLi in hexane (1.74 ml, 4.34 mmol) and dimesitylboron fluoride (**2**) (1.16 g, 4.34 mmol) as described above for compound **5**. Chromatography on silica gel with pentane afforded the product as a white solid (1.96 g, 2.99 mmol, 69%). ¹H NMR (400 MHz, CDCl₃): δ [ppm] 7.65 (d, *J* = 1.1 Hz, 2 H), 7.38 (t, *J* = 1.1 Hz, 1 H), 6.75 (s, 8 H), 2.28 (s, 12 H), 1.94 (s, 24 H).

N-ph-B. Compound **3** (0.20 g, 0.51 mmol),¹¹ dianisylamine (**7**) (0.11 g, 0.47 mmol), NaO^tBu (0.82 g, 8.5 mmol), Pd(dba)₂ (23 mg, 0.04 mmol), and (HP^tBu₃)BF₄ (8.3 mg, 0.04 mmol) were dissolved in dry de-oxygenated toluene (15 ml) under N₂. The mixture was reacted at 120 °C for 2 h. Brine (100 ml) was added to the cooled solution, and the aqueous phase was extracted with CH₂Cl₂ (3×50 ml). The solvents were evaporated after drying over Na₂SO₄, and the crude product was purified by column chromatography on silica gel. The eluent was an 18:1 (v:v) mixture of pentane and EtOAc. The pure product was obtained as a bright yellow solid (0.24 g, 0.43 mmol, 92%). ¹H NMR (250 MHz, DMSO-*d*₆): δ [ppm] 7.21-7.10 (m, 6 H), 6.99-6.91 (m, 4 H), 6.77 (s, 4 H), 6.61 (d, *J* = 8.7 Hz, 2 H), 3.74 (s, 6 H), 2.22 (s, 6 H), 1.97 (s, 12 H). ¹³C NMR (100 MHz, DMSO-*d*₆): δ [ppm] 156.7, 152.1, 141.4, 139.7, 138.5, 138.2, 137.2, 134.3, 128.1, 127.9, 115.3, 115.0, 55.2, 23.0, 20.7. HRMS (ESI TOF) *m/z*: [M]⁺ Calcd for C₃₈H₄₀NO₂B 553.3153; Found 553.3147. Anal. Calcd for C₃₈H₄₀NO₂B: C, 82.45; H, 7.28; N, 2.53. Found: 82.05; H, 7.29; N, 2.40.

N₃-ph-B. Compound **3** (72 mg, 0.18 mmol),¹¹ oligotriarylamine **8** (100 mg, 0.16 mmol), NaO^tBu (308 mg, 3.2 mmol), Pd(dba)₂ (12 mg, 0.02 mmol), and (HP^tBu₃)BF₄ (4.6 mg, 0.02 mmol) were dissolved in dry and de-oxygenated toluene (100 ml) under N₂. The mixture was refluxed for 1.25 h and then cooled to room temperature. Brine (100 ml) was added and the aqueous phase was extracted with CH₂Cl₂ (3×50 ml). The combined organic phases were dried over Na₂SO₄

1
2
3 and evaporated. Chromatography on silica gel column with a 1:1 (v:v) mixture of pentane and
4
5 CH₂Cl₂ followed by recrystallization from acetone afforded the pure product as a bright yellow
6
7 solid (117 mg, 0.12 mmol, 77%). ¹H NMR (400 MHz, acetone-d₆): δ [ppm] 7.31-7.25 (m, 2 H),
8
9 7.11-7.02 (m, 12 H), 6.93-6.84 (m, 12 H), 6.82-6.76 (m, 6 H), 3.78 (s, 12 H), 2.25 (s, 6 H), 2.04
10
11 (s, 12 H). ¹³C NMR (100 MHz, C₆D₆): δ [ppm] 156.2, 152.5, 146.1, 142.4, 141.2, 140.7, 139.5,
12
13 137.6, 136.2, 128.4, 127.6, 126.5, 125.7, 121.9, 117.1, 114.9, 54.7, 23.6, 21.0. HRMS (ESI TOF)
14
15 m/z: [M]⁺ Calcd for C₆₄H₆₂N₃O₄B 947.4838; Found 947.4834. Anal. Calcd for
16
17 C₆₄H₆₂N₃O₄B·0.5H₂O: C, 80.32; H, 6.64; N, 4.39. Found: 80.36; H, 6.81; N, 4.46. Water is also
18
19 detected in the ¹H NMR spectrum, see Supporting Information.
20
21
22
23

24
25 N₃-ph-B₂. Compound **6** (118 mg, 0.18 mmol),¹³ oligotriarylamine **8** (100 mg, 0.16 mmol),
26
27 NaO^tBu (308 mg, 3.2 mmol), Pd(dba)₂ (12 mg, 0.02 mmol), and (HP^tBu₃)BF₄ (4.6 mg, 0.02
28
29 mmol) were dissolved in dry de-oxygenated toluene (10 ml) under N₂. The mixture was refluxed
30
31 for 1 h and then cooled to room temperature. Brine (100 ml) was added, and after phase
32
33 separation the aqueous layer was extracted with CH₂Cl₂ (3×50 ml). After drying over Na₂SO₄
34
35 and evaporation of the solvents, the crude product was purified on silica gel column. First the
36
37 eluent was a 1:1 (v:v) mixture of pentane and CH₂Cl₂, then pure CH₂Cl₂ was used. The pure
38
39 product crystallized when dropping a concentrated CH₂Cl₂ solution into methanol (120 mg, 0.10
40
41 mmol, 63%). ¹H NMR (400 MHz, acetone-d₆): δ [ppm] 7.27 (d, *J* = 1.1 Hz, 2 H), 7.22 (t, *J* = 1.1
42
43 Hz, 1 H), 6.97-6.92 (m, 8 H), 6.90-6.84 (m, 12 H), 6.79-6.74 (m, 12 H), 3.79 (s, 12 H), 2.22 (s,
44
45 12 H), 1.98 (s, 24 H). ¹³C NMR (100 MHz, acetone-d₆): δ [ppm] 156.8, 145.1, 142.8, 142.3,
46
47 141.4, 139.7, 138.4, 136.8, 134.2, 129.2, 127.8, 126.7, 125.7, 123.6, 120.1, 115.6, 55.9, 23.8,
48
49 21.6. HRMS (ESI TOF) m/z: [M]⁺ Calcd for C₈₂H₈₃N₃O₄B₂ 1195.6588; Found 1195.6576. Anal.
50
51
52
53
54
55
56
57
58
59
60

1
2
3
4
5
6
7
8
9
10
11
12
13
14
15
16
17
18
19
20
21
22
23
24
25
26
27
28
29
30
31
32
33
34
35
36
37
38
39
40
41
42
43
44
45
46
47
48
49
50
51
52
53
54
55
56
57
58
59
60

Calcd for $C_{82}H_{83}N_3O_4B_2 \cdot 0.5H_2O$: C, 81.72; H, 7.02; N, 3.49. Found: 81.83; H, 6.95; N, 3.44.

Water is also detected in the 1H NMR spectrum, see Supporting Information.

Compound **11**.¹⁴ 4-Bromo-1-iodobenzene (**9**) (2.00 g, 7.06 mmol) and trimethylsilyl acetylene (**10**) (1.10 ml, 7.78 mmol) were dissolved in dry Et_3N (30 ml) under N_2 . $PdCl_2(PPh_3)_2$ (98 mg, 0.14 mmol) and CuI (53 mg, 0.28 mmol) were added and the reaction mixture was heated to 100 $^{\circ}C$ for 30 min. After cooling to room temperature, saturated aqueous NH_4Cl solution (100 ml) was added and the product was extracted with CH_2Cl_2 (3 \times 50 ml). The organic phases were dried over Na_2SO_4 and evaporated. Chromatography on silica gel column with pentane gave a white solid (1.80 g, 7.11 mmol, ~100%). 1H NMR (400 MHz, $CDCl_3$): δ [ppm] 7.45-7.41 (m, 2 H), 7.33-7.30 (m, 2 H), 0.25 (s, 9 H).

Compound **12**.¹⁵ Compound **11** (1.00 g, 4.0 mmol),¹⁴ dianisylamine (**7**) (725 mg, 3.2 mmol), NaO^tBu (6.3 mg, 65.6 mmol), $Pd(dba)_2$ (190 mg, 0.3 mmol), and P^tBu_3 (0.98 ml, 0.3 mmol) were dissolved in dry de-oxygenated toluene (60 ml) under N_2 . The mixture was refluxed for 30 h, and after cooling to room temperature brine (100 ml) was added. After phase separation the aqueous layer was extracted with CH_2Cl_2 (3 \times 50 ml), and the combined organic phases were dried over Na_2SO_4 . Column chromatography on silica gel with a 1:3 (v:v) mixture of pentane and CH_2Cl_2 afforded the pure product as a yellow solid (810 mg, 2.0 mmol, 64%). 1H NMR (250 MHz, acetone- d_6): δ [ppm] 7.27-7.19 (m, 2 H), 7.12-7.05 (m, 4 H), 6.97-6.89 (m, 4 H), 6.76-6.68 (m, 2 H), 3.80 (s, 6 H), 0.2 (s, 9 H).

Compound **13**. Compound **11** (150 mg, 0.59 mmol), oligotriarylamine **8** (308 mg, 0.49 mmol), NaO^tBu (942 mg, 9.80 mmol), $Pd(dba)_2$ (28 mg, 0.05 mmol), and $(HP^tBu_3)BF_4$ (14 mg, 0.05 mmol) were dissolved in dry and de-oxygenated toluene (15 ml). The mixture was refluxed under N_2 for 20 h. Brine (100 ml) was added to the cooled mixture, and the aqueous phase was

1
2
3 extracted with CH₂Cl₂ (3×50 ml). After drying over Na₂SO₄ and evaporation of the solvents, the
4
5 crude product was purified by column chromatography on silica gel using CH₂Cl₂ as the eluent.
6
7
8 The pure product was obtained as a yellow oil which solidified over time (290 mg, 0.36 mmol,
9
10 74%). ¹H NMR (400 MHz, acetone-d₆): δ [ppm] 7.25-7.23 (m, 2 H), 7.08-7.06 (m, 8 H), 6.99-
11
12 6.97 (m, 4 H), 6.90-6.82 (m, 14 H), 3.78 (s, 12 H), 0.19 (s, 9 H).
13
14

15 Compound **14**.¹⁵ Compound **12** (0.80 g, 2.0 mmol) was dissolved in THF (40 ml) under N₂,
16
17 and TBAF solution in methanol (18.0 ml, 5.4 mmol) was added dropwise. The reaction mixture
18
19 was stirred at room temperature for 1 h, and then the solvents were evaporated. The solid residue
20
21 was taken up in EtOAc and washed with water (3×100 ml). After drying over Na₂SO₄ and
22
23 evaporating the solvent, the pure product was obtained as a yellow solid (0.65 g, 2.0 mmol,
24
25 99%). ¹H NMR (250 MHz, CDCl₃): δ [ppm] 7.30-7.23 (m, 2 H), 7.11-7.01 (m, 4 H), 6.89-6.76
26
27 (m, 6 H), 3.80 (s, 6 H).
28
29
30
31

32 Compound **15**. Compound **13** (300 mg, 0.38 mmol) was dissolved in dry THF (10 ml) under
33
34 N₂. TBAF solution in THF (1.40 ml, 0.38 mmol) was added dropwise, and the reaction mixture
35
36 was stirred at room temperature for 1.5 h. After removal of THF, the solid residue was taken up
37
38 in EtOAc (100 ml) and washed with water. The organic phases were dried over Na₂SO₄ and
39
40 evaporated to dryness. This afforded the pure product as a yellow solid (250 mg, 0.35 mmol,
41
42 91%). ¹H NMR (400 MHz, C₆D₆): δ [ppm] 7.38-7.36 (m, 2 H), 7.12-7.07 (m, 8 H), 7.05-6.97 (m,
43
44 10 H), 6.73-6.68 (m, 8 H), 3.29 (s, 12 H), 2.76 (s, 1 H).
45
46
47

48 N-phCC-B.^{9b} Compound **3** (270 mg, 0.67 mmol) and compound **14** (200 mg, 0.61 mmol) were
49
50 suspended in dry Et₃N (15 ml) under N₂. CuI (4.5 mg, 0.02 mmol) and PdCl₂(PPh₃)₂ (8.4 mg,
51
52 0.01 mmol) were added, and the reaction mixture was refluxed for 30 h. After cooling to room
53
54 temperature, saturated aqueous NH₄Cl solution (100 ml) was added, and the aqueous phase was
55
56
57
58
59
60

1
2
3 extracted with CH₂Cl₂ (3×50 ml). After drying over Na₂SO₄ and evaporation of the solvents, the
4
5 crude product was purified by chromatography on silica gel using an 18:1 (v:v) mixture of
6
7 pentane and EtOAc as the eluent. Subsequent recrystallization by dropping a concentrated
8
9 CH₂Cl₂ solution into methanol afforded the pure product as a yellow solid (172 mg, 0.26 mmol,
10
11 43%). ¹H NMR (250 MHz, acetone-d₆): δ [ppm] 7.49 (ABq, 4 H, Δδ_{AB} = 0.04, J_{AB} = 8.8 Hz),
12
13 7.38-7.32 (m, 2 H), 7.16-7.09 (m, 4 H), 6.99-6.91 (m, 4 H), 6.85 (s, 4 H), 6.81-6.75 (m, 2 H),
14
15 3.81 (s, 6 H), 2.29 (s, 6 H), 2.00 (s, 12 H). ¹³C NMR (100 MHz, acetone-d₆): δ [ppm] 158.9,
16
17 151.5, 147.3, 143.4, 142.5, 141.6, 140.8, 138.0, 134.5, 132.7, 130.2, 129.5, 129.4, 120.0, 116.9,
18
19 114.8, 94.7, 90.1, 56.9, 24.8, 22.4. HRMS (ESI TOF) m/z: [M]⁺ Calcd for C₄₆H₄₄NO₂B
20
21 653.3467; Found 653.3456. Anal. Calcd for C₄₆H₄₄NO₂B·0.5H₂O: C, 83.37; H, 6.84; N, 2.11.
22
23 Found: 83.74; H, 6.83; N, 2.20. Water is also detected in the ¹H NMR spectrum, see Supporting
24
25 Information.
26
27
28
29
30
31

32 N₃-phCC-B. Compound **15** (217 mg, 0.30 mmol) and compound **3** (100 mg, 0.25 mmol) were
33
34 dissolved in dry Et₃N (10 ml) under N₂ atmosphere. PdCl₂(PPh₃)₂ (3.5 mg, 0.005 mmol) and CuI
35
36 (1.9 mg, 0.01 mmol) were added, and the reaction mixture was refluxed overnight. After cooling
37
38 to room temperature, saturated aqueous NH₄Cl solution was added, and the product was
39
40 extracted with CH₂Cl₂ (3×50 ml). The combined organic phases were dried over Na₂SO₄ and
41
42 evaporated. Chromatography on silica gel column with a 1:2 (v:v) mixture of pentane and
43
44 CH₂Cl₂ afforded the product as an orange oil (110 mg, 0.11 mmol, 42%). When drops of a
45
46 concentrated solution of this oil in CH₂Cl₂ were added to water, an orange solid was obtained. ¹H
47
48 NMR (400 MHz, acetone-d₆): δ [ppm] 7.48 (ABq, 4 H, Δδ_{AB} = 0.02, J_{AB} = 8.0 Hz), 7.37-7.33 (m,
49
50 2 H), 7.07-7.00 (m, 12 H), 6.91-6.84 (m, 18 H), 3.77 (s, 12 H), 2.28 (s, 6 H), 2.00 (s, 12 H). ¹³C
51
52 NMR (100 MHz, acetone-d₆): δ [ppm] 157.2, 150.2, 146.7, 146.4, 142.5, 141.9, 140.4, 139.8,
53
54
55
56
57
58
59
60

1
2
3 139.1, 137.1, 129.3, 127.9, 127.5, 122.4, 119.8, 115.7, 114.1, 93.8, 89.3, 55.9, 23.9, 21.4. HRMS
4
5 (ESI TOF) m/z: [M]⁺ Calcd for C₇₂H₆₆N₃O₄B 1047.5152; Found 1047.5127. Anal. Calcd for
6
7 C₇₂H₆₆N₃O₄B: C, 82.51; H, 6.35; N, 4.01. Found: 82.45; H, 6.65; N, 3.80.

8
9
10 N₃-phCC-B₂. Compound **15** (180 mg, 0.25 mmol) and compound **6** (195 mg, 0.29 mmol)¹³
11
12 were suspended in dry Et₃N (10 ml) under N₂. PdCl₂(PPh₃)₂ (3.5 mg, 0.005 mmol) and CuI (1.9
13
14 mg, 0.01 mmol) were added, and the mixture was reacted at reflux overnight. After cooling to
15
16 room temperature, saturated aqueous NH₄Cl solution (100 ml) was added and the product was
17
18 extracted with CH₂Cl₂ (3×50 ml). The combined organic phases were dried over Na₂SO₄ and
19
20 evaporated. Column chromatography on silica gel with a 1:2 (v:v) mixture of pentane and
21
22 CH₂Cl₂ gave a yellow oil. When drops of a concentrated solution of this oil in CH₂Cl₂ were
23
24 added to methanol, the product was obtained as an orange solid (110 mg, 0.09 mmol, 34%). ¹H
25
26 NMR (400 MHz, acetone-d₆): δ [ppm] 7.66 (d, *J* = 1.3 Hz, 2 H), 7.54 (t, *J* = 1.3 Hz, 1 H), 7.25
27
28 (d, *J* = 8.7 Hz, 2 H), 7.07-7.01 (m, 8 H), 6.98 (d, *J* = 8.7 Hz, 4 H), 6.92-6.68 (m, 8 H), 6.86-6.81
29
30 (m, 6 H), 6.79 (s, 8 H), 3.77 (s, 12 H), 2.24 (s, 12 H), 1.97 (s, 24 H). ¹³C NMR (100 MHz,
31
32 acetone-d₆): δ [ppm] 157.2, 149.9, 148.0, 146.7, 142.5, 142.2, 141.9, 141.5, 140.5, 140.2, 133.4,
33
34 129.3, 127.7, 127.4, 124.8, 122.4, 119.8, 115.8, 115.2, 114.2, 91.6, 88.9, 55.9, 23.9, 21.5. HRMS
35
36 (ESI TOF) m/z: [M]⁺ Calcd for C₉₀H₈₇N₃O₄B₂ 1295.6902; Found 1295.6878. Anal. Calcd for
37
38 C₉₀H₈₇N₃O₄B₂·0.5H₂O: C, 82.81; H, 6.80; N, 3.22. Found: 82.64; H, 6.74; N, 2.94. Water is also
39
40 detected in the ¹H NMR spectrum, see Supporting Information.

41
42
43
44
45
46
47
48 NMR spectroscopy, ESI-HRMS, elemental analysis, cyclic voltammetry, optical absorption
49
50 and luminescence spectroscopy occurred using the same equipment as described in detail in a
51
52 recent publication.^{10c} Fluorescence lifetime measurements were performed using a commercial
53
54
55
56
57
58
59
60

1
2
3 fluorescence lifetime spectrometer. Absolute photoluminescence quantum yields were measured
4
5 on a commercial absolute photoluminescence quantum yield measurement system.
6
7
8
9

10
11 SUPPORTING INFORMATION AVAILABLE
12

13
14 ^1H and $^1\text{H}/^{13}\text{C}$ -HMBC NMR spectra, ESI-HRMS spectra, additional electrochemical and optical
15
16 spectroscopic data. This material is available free of charge via the Internet at <http://pubs.acs.org>.
17
18
19

20
21
22 AUTHOR INFORMATION
23

24
25 **Corresponding Author**
26

27 *E-mail: oliver.wenger@unibas.ch
28
29
30
31
32

33
34 ACKNOWLEDGMENT
35

36
37
38 This work was supported by the Swiss National Science Foundation through grant number
39
40 200021_146231/1 and by the Deutsche Forschungsgemeinschaft through grant number
41
42 WE4815/3-1.
43
44
45
46
47
48

49
50 REFERENCES
51

52
53
54 (1) Hagfeldt, A.; Boschloo, G.; Sun, L. C.; Kloo, L.; Pettersson, H., *Chem. Rev.* **2010**, *110*,
55
56 6595.
57
58
59
60

1
2
3 (2) (a) Marder, S. R.; Cheng, L. T.; Tiemann, B. G.; Friedli, A. C.; Blanchard-Desce, M.;
4 Perry, J. W.; Skindhoj, J., *Science* **1994**, *263*, 511. (b) Kim, H. M.; Cho, B. R., *Acc. Chem. Res.*
5
6 **2009**, *42*, 863.
7
8

9
10
11 (3) Hide, F.; DiazGarcia, M. A.; Schwartz, B. J.; Heeger, A. J., *Acc. Chem. Res.* **1997**, *30*,
12
13 430.
14

15
16
17 (4) Glasbeek, M.; Zhang, H., *Chem. Rev.* **2004**, *104*, 1929.
18

19
20 (5) (a) Entwistle, C. D.; Marder, T. B., *Angew. Chem. Int. Ed.* **2002**, *41*, 2927. (b) Elbing,
21
22 M.; Bazan, G. C., *Angew. Chem. Int. Ed.* **2008**, *47*, 834. (c) Yamaguchi, S.; Wakamiya, A., *Pure*
23
24 *Appl. Chem.* **2006**, *78*, 1413. (d) Jäkle, F., *Chem. Rev.* **2010**, *110*, 3985. (e) Lorbach, A.; Bolte,
25
26 M.; Li, H. Y.; Lerner, H. W.; Holthausen, M. C.; Jäkle, F.; Wagner, M., *Angew. Chem. Int. Ed.*
27
28 **2009**, *48*, 4584.
29
30

31
32 (6) (a) Wade, C. R.; Broomsgrove, A. E. J.; Aldridge, S.; Gabbai, F. P., *Chem. Rev.* **2010**,
33
34 *110*, 3958. (b) Broomsgrove, A. E. J.; Addy, D. A.; Bresner, C.; Fallis, I. A.; Thompson, A. L.;
35
36 Aldridge, S., *Chem. Eur. J.* **2008**, *14*, 7525. (c) Hudnall, T. W.; Chiu, C. W.; Gabbai, F. P., *Acc.*
37
38 *Chem. Res.* **2009**, *42*, 388. (d) Yamaguchi, S.; Akiyama, S.; Tamao, K., *J. Am. Chem. Soc.* **2000**,
39
40 *122*, 6335. (e) Liu, X. Y.; Bai, D. R.; Wang, S. N., *Angew. Chem. Int. Ed.* **2006**, *45*, 5475. (f)
41
42 Sun, Y.; Ross, N.; Zhao, S. B.; Huszarik, K.; Jia, W. L.; Wang, R. Y.; Macartney, D.; Wang, S.
43
44 N., *J. Am. Chem. Soc.* **2007**, *129*, 7510.
45
46
47

48
49
50 (7) Yamaguchi, S.; Shirasaka, T.; Akiyama, S.; Tamao, K., *J. Am. Chem. Soc.* **2002**, *124*,
51
52 8816.
53
54
55
56
57
58
59
60

1
2
3 (8) (a) Zhao, C. H.; Wakamiya, A.; Inukai, Y.; Yamaguchi, S., *J. Am. Chem. Soc.* **2006**, *128*,
4 15934. (b) Zhou, G.; Baumgarten, M.; Müllen, K., *J. Am. Chem. Soc.* **2008**, *130*, 12477. (c)
5 Hudson, Z. M.; Wang, S. N., *Acc. Chem. Res.* **2009**, *42*, 1584. (d) Schmidt, H. C.; Reuter, L. G.;
6 Hamacek, J.; Wenger, O. S., *J. Org. Chem.* **2011**, *76*, 9081. (e) Chen, P. K.; Jäkle, F., *J. Am.*
7 *Chem. Soc.* **2011**, *133*, 20142. (f) Mengel, A. K. C.; He, B.; Wenger, O. S., *J. Org. Chem.* **2012**,
8 *77*, 6545. (g) Entwistle, C. D.; Marder, T. B., *Chem. Mat.* **2004**, *16*, 4574. (h) Pron, A.; Zhou, G.;
9 Norouzi-Arasi, H.; Baumgarten, M.; Müllen, K., *Org. Lett.* **2009**, *11*, 3550.

10
11
12
13
14
15
16
17
18
19
20
21 (9) (a) Chen, P. K.; Lalancette, R. A.; Jäkle, F., *Angew. Chem. Int. Ed.* **2012**, *51*, 7994. (b)
22 Steeger, M.; Lambert, C., *Chem.-Eur. J.* **2012**, *18*, 11937.

23
24
25
26 (10) (a) Hirao, Y.; Ito, A.; Tanaka, K., *J. Phys. Chem. A* **2007**, *111*, 2951. (b) Karlsson, S.;
27 Boixel, J.; Pellegrin, Y.; Blart, E.; Becker, H. C.; Odobel, F.; Hammarström, L., *J. Am. Chem.*
28 *Soc.* **2010**, *132*, 17977. (c) Bonn, A. G.; Neuburger, M.; Wenger, O. S., *Inorg. Chem.* **2014**, *53*,
29 11075.

30
31
32
33
34
35
36
37 (11) Xu, X. F.; Ye, S. H.; He, B. R.; Chen, B.; Xiang, J. Y.; Zhou, J.; Lu, P.; Zhao, Z. J.; Qiu,
38 H. Y., *Dyes Pigments* **2014**, *101*, 136.

39
40
41
42 (12) Rao, Y.-L.; Schoenmakers, D.; Chang, Y.-L.; Lu, J.-S.; Lu, Z.-H.; Kang, Y.; Wang, S.,
43 *Chem. Eur. J.* **2012**, *18*, 11306.

44
45
46
47 (13) Cunningham, A. F.; Kunz, M.; Kura, H. Photoinitiators comprising boranes and electron
48 donors, Eur. Pat. Appl. 2002, EP 1203999 A2 20020508.

49
50
51
52
53 (14) Florian, A.; Mayoral, M. J.; Stepanenko, V.; Fernandez, G., *Chem. Eur. J.* **2012**, *18*,
54 14957.
55
56
57
58
59
60

1
2
3 (15) (a) Zieschang, F.; Schreck, M. H.; Schmiedel, A.; Holzapfel, M.; Klein, J. H.; Walter, C.;
4 Engels, B.; Lambert, C., *J. Phys. Chem. C* **2014**, *118*, 27698. (b) Lambert, C.; Nöll, G.;
5
6 Schmälzlin, E.; Meerholz, K.; Bräuchle, C., *Chem. Eur. J.* **1998**, *4*, 2129.
7
8

9
10
11 (16) (a) Sreenath, K.; Thomas, T. G.; Gopidas, K. R., *Org. Lett.* **2011**, *13*, 1134. (b) Kaim, W.;
12 Schulz, A., *Angew. Chem. Int. Ed.* **1984**, *23*, 615.
13
14

15
16
17 (17) (a) Stahl, R.; Lambert, C.; Kaiser, C.; Wortmann, R.; Jakober, R., *Chem.-Eur. J.* **2006**,
18 *12*, 2358. (b) Bai, D. R.; Liu, X. Y.; Wang, S. I., *Chem.-Eur. J.* **2007**, *13*, 5713.
19
20

21
22 (18) Reichardt, C., *Chem. Rev.* **1994**, *94*, 2319.
23
24

25
26 (19) (a) Lippert, E., *Z. Naturforsch. A* **1955**, *10*, 541. (b) Mataga, N.; Kaifu, Y.; Koizumi, M.,
27 *Bull. Chem. Soc. Jpn.* **1955**, *28*, 690.
28
29

30
31 (20) Onsager, L., *J. Am. Chem. Soc.* **1936**, *58*, 1486.
32
33

34 (21) Suppan, P., *Chem. Phys. Lett.* **1983**, *94*, 272.
35
36

37 (22) Caspar, J. V.; Meyer, T. J., *J. Phys. Chem.* **1983**, *87*, 952.
38
39

40 (23) Zhang, Z.; Edkins, R. M.; Nitsch, J.; Fucke, K.; Steffen, A.; Longobardi, L. E.; Stephan,
41 D. W.; Lambert, C.; Marder, T. B., *Chem. Sci.* **2015**, *6*, 308.
42
43
44
45
46
47
48
49
50
51
52
53
54
55
56
57
58
59
60